ELSEVIER

applied surface science

www.elsevier.nl/locate/apsusc

Decomposition of the sulfates of copper, iron (II), iron (III), nickel, and zinc: XPS, SEM, DRIFTS, XRD, and TGA study

Ranjani V. Siriwardane [a,*], James A. Poston Jr. [a], Edward P. Fisher [a], Ming-Shing Shen [a], Angela L. Miltz [b]

[a] *U.S. Department of Energy, Federal Energy Technology Center, P.O. Box 880, 3610 Collins Ferry Road, Morgantown, WV 26507-0880, USA*

[b] *EG&G-TSWV, 3610 Collins Ferry Road, Morgantown, WV 26507-0880, USA*

Received 16 February 1999; accepted 2 July 1999

Abstract

The bulk and surface characteristics during decomposition of the transition metal sulfates of copper, iron (II), iron (III), nickel, and zinc are investigated utilizing various spectroscopic techniques. An oxidized form of sulfur was detected on the surface during decomposition of all metal sulfate samples, except zinc sulfate. Surface characteristics were not necessarily representative of the bulk characteristics. Oxy-sulfate was observed with copper sulfate only. Lower decomposition temperatures were observed in vacuum as compared to those at atmospheric pressure. Uniform sulfur distribution was observed across sample cross sections. Analysis consisted of Scanning electron microscopy/X-ray microanalysis, X-ray photoelectron spectroscopy, diffuse reflectance infrared Fourier transform spectroscopy, thermogravimetric analysis, and X-ray diffraction.

Keywords: Transition metal oxide; Fuel gas; Copper

1. Introduction

Transition metal oxides have been utilized as high temperature regenerable sorbents for removal of hydrogen sulfide from fuel gas obtained from coal gasification [1–6]. The performance of these sorbents depends both on their sulfidation ability and their regenerability. Regeneration of the sulfided sorbents is usually performed utilizing oxygen. In addition to SO_2 (desirable product) formation, metal sulfate is also formed during regeneration, which has a negative effect on the sorbent durability [7–10]. Thus, it is important to understand the decomposition of the undesirable metal sulfate. Decomposition of transition metal sulfates have been studied by various researchers [11–20]. Most of these studies were conducted with thermogravimetric analysis (TGA), gravimetric torsion-effusion, and differential thermal analysis (DTA). Oxy-sulfate has been identified as an intermediate during the decomposition of zinc sulfate and copper sulfate. Kinetic parameters have been determined and decomposition temperatures have also been identified during these studies. However, none of these studies dealt with surface characterization or systematic identification of the oxidation states of the elements and different sulfur species

* Corresponding author

formed during the decomposition. The relationship between bulk and surface properties during decomposition has not been investigated.

In this study, research focused toward understanding the decomposition temperatures and both bulk and surface species formed during the decomposition of sulfates of copper, iron(II), iron(III), nickel, and zinc. Bulk and surface decomposition data were then analyzed and compared. The analytical techniques employed to conduct this study include X-ray Photoelectron Spectroscopy (XPS), Scanning Electron Microscopy/X-ray microanalysis (SEM/EDS), Thermogravimetric Analysis (TGA), X-ray Diffraction (XRD) and Diffuse Reflectance Infrared Fourier Transform Spectroscopy (DRIFTS).

2. Experimental

$NiSO_4 \cdot 6H_2O$, $CuSO_4 \cdot XH_2O$, $ZnSO_4 \cdot XH_2O$, $FeSO_4 \cdot 7H_2O$, $Fe_2(SO_4)_3$ were purchased from Alfa, Johnson Matthey. Copper, iron (II), iron (III), and zinc sulfates were puratronic grade with a purity of 99.999%. Two grades of nickel sulfate were used in these series of experiments, puratronic and assay, 99.9985% and $>98\%$ purity respectively. The puratronic grade nickel sulfate was used in all experiments except X-ray mapping. In the X-ray mapping, the larger crystalline form of the assay grade nickel sulfate proved more suitable. Results of TGA studies on the $CuSO_4 \cdot XH_2O$ sample indicated that in the initial hydrated form, $X \cong 4$, while that for $ZnSO_4 \cdot XH_2O$ indicated that in the initial hydrated form, $X \cong 2$. Sample heating was accomplished by placing the metal sulfate(s), contained in a ceramic crucible, into a pre-heated muffle furnace for 90 min. The metal sulfate samples were heated to 300°C, 500°C, and following 500°C, in 50°C increments up to the point of complete or near complete sulfate decomposition (0°C = 273.15 Kelvin (K)). The fresh metal sulfate samples served as the reference material. Upon being removed from the furnace, the samples were sealed in glass vials, where they were allowed to cool. Vials were opened immediately prior to preparation for the analysis. Regeneration of the desulfurization sorbents during reactor testing is conducted utilizing oxygen and nitrogen at or above atmospheric pressures. The sulfate decomposition was conducted in a muffle furnace in order to better simulate the conditions in a reactor system, as opposed to that found in vacuum systems. During DRIFTS studies the metal sulfates were decomposed in situ, with the diffuse reflectance cell pressure at 10^{-5} Torr (1.3×10^{-3} Pa). This allowed not only for in situ measurements, but also the investigation of how vacuum affects the decomposition.

X-ray photoelectron spectroscopy (XPS) spectra were recorded with a Physical Electronics Model SAM 590 equipped with a cylindrical mirror analyzer and a 15 kV X-ray source from Physical Electronics. The system was routinely operated within a pressure range of 10^{-9}–10^{-8} Torr (1.3×10^{-7} to 1.3×10^{-6} Pa). The instrument was calibrated using the photoemission lines E_B (Cu $2p_{3/2}$) = 932.4 eV and E_B (Au $4f_{7/2}$) = 83.8 eV [21]. The binding energies were referenced to the C(1s) level at 284.6 eV for adventitious carbon. All intensities reported are experimentally determined peak areas divided by the instrumental sensitivity factors. Three sets of spectra were obtained at each temperature. The intensity and binding energy values reported at a given temperature are the average of values obtained from the three spectra.

Thermogravimetric Analysis was conducted using a TA Instruments 951 Thermogravimetric Analyzer (TGA). The 951 model is a horizontal design TGA. Each test was conducted with a flow rate of 50 cc/min of nitrogen through the furnace and balance sides of the TGA. Approximately 25–30 mg of sample was weighed onto a platinum pan for each sulfate decomposition test. The sample was then held at ambient conditions for 40 min before it was heated at a rate of 5°C/min to 200°C where the temperature was held for 1 h. The sample was then heated at the same heating rate to 300°C and held for 15 min. This step was then repeated, raising the temperature in 100°C increments and holding for 15 min until a temperature of 900°C was reached (i.e., 400°C, 500°C, 600°C, 700°C, 800°C, and 900°C.) The final step in the decomposition program was to increase the temperature to 950°C at a rate of 5°C/min where the temperature was held for 15 min.

X-ray microanalysis was carried out using a JEOL model 840-A scanning electron microscope (SEM) which was routinely operated within a pressure range

of 10^{-7} to 10^{-6} Torr (1.3×10^{-5} to 1.3×10^{-4} Pa). The JEOL-840A SEM was interfaced to a Noran Instruments X-ray microanalysis system and a TN-5600 PAC system. The JEOL-840A is equipped with a high sensitivity, solid state, annular backscatter electron detector, an ET-type secondary electron detector, and a Noran Instruments Micro-Z series energy dispersive spectrometer (EDS). The energy dispersive spectrometer was operated in the Beryllium window mode. Based on the manganese (Alfa Puratronic) $K\alpha$ spectral line, the energy dispersive spectrometer had a detector resolution of 148 eV. The microanalysis system, prior to analysis, was calibrated using a copper metal reference standard, with the centroid of the $K\alpha$ spectral peak being referenced to the energy value of 8.046 keV. Initial spectra were obtained on a Noran Instruments TN-8502 switcher system and analyzed using the Noran Instruments MicroQ quantitative analysis program, while later spectra were obtained on a Noran Instruments Voyager-4 X-ray microanalysis unit and analyzed using the Noran Instruments Voyager-4 quantitative analysis program. Spectral acquisition time was 120 s and a minimum of 5 spectra were obtained for each sample at an accelerating voltage of 15 kV. In all spectral analysis, oxygen was calculated by difference and matrix corrections were made using the Phi-ro-z ($\phi\rho Z$) matrix correction program. Sulfur to metal ratios ($S/[M]$) were based on the calculated weight percentages. For standard microanalysis, the sample material was pressed into a pellet on the order of ≤ 1 mm thick and 1–2 cm in diameter utilizing a Carver Model-C laboratory press. The X-ray analysis results are considered to be semi-quantitative due to the geometric effect caused by the sample surface. Although matrix correction programs were designed for flat, non-porous (ideal) samples placed at known angles to the electron beam [22], a significant amount of the error that would normally be encountered in the analysis of particles and rough surface specimens was statistically eliminated due to the ratioing of the compositional results.

Diffuse reflectance infrared Fourier transform spectroscopy (DRIFTS) was carried out using a Mattson Polaris infrared Fourier transform spectrometer equipped with a Harrick Scientific diffuse reflectance attachment. The diffuse reflectance cell was operated at pressure of 10^{-5} Torr (1.3×10^{-3} Pa). The sample was brought up to the desired temperature and then monitored until the degassing was complete and the system pressure returned to the operating pressure. Typically, the time for the system to return to its operating pressure was on the order of 1 to 1.5 h.

X-ray Diffraction was carried out using a Phillips PW 1800 X-ray Diffraction (XRD) system. The XRD system was equipped with a single crystal monochrometer.

3. Results and discussion

3.1. TGA analysis

TGA analysis was conducted to understand the bulk decomposition properties of the sulfates. The TGA data for the decomposition of the sulfates are shown in Fig. 1. The initial decomposition temperature for zinc sulfate was observed around 700°C with a sharp decrease in weight being observed around 800°C. An additional sharp decrease in weight was observed between 800°C and 862°C. Literature values [12–14,18] for the decomposition temperatures of $ZnSO_4$ range from 610°C to 846°C. Several researchers identified the oxysulfate intermediate as the initial decomposition product. Mu and Perimutter [13] indicated that the anhydrous sulfate begins to convert to oxysulfate, $ZnO\cdot 2ZnSO_4$, at 590°C, with this process being complete at 712°C. The final conversion of the sulfate to ZnO, as reported by Mu and Perimutter [13], was complete at 837°C. The initial decomposition temperature of 600°C observed in this study is very close to the value obtained by Mu and Perimutter [13]. The TGA decomposition profile for $ZnSO_4$ reached a minimum at 890°C and maintained that minimum through the maximum temperature of 950°C. The weight loss observed during decomposition was approximately 49%, corresponding to a decomposition product of ZnO. As stated above, in the case of Mu and Perimutter [13], complete decomposition of $ZnSO_4$ to ZnO was achieved at 837°C, a temperature difference of approximately 6% below that obtained in these experiments. Platinum sample boats have been shown to have a catalytic effect on decomposition [14], however in these experiments this catalytic effect was not observed.

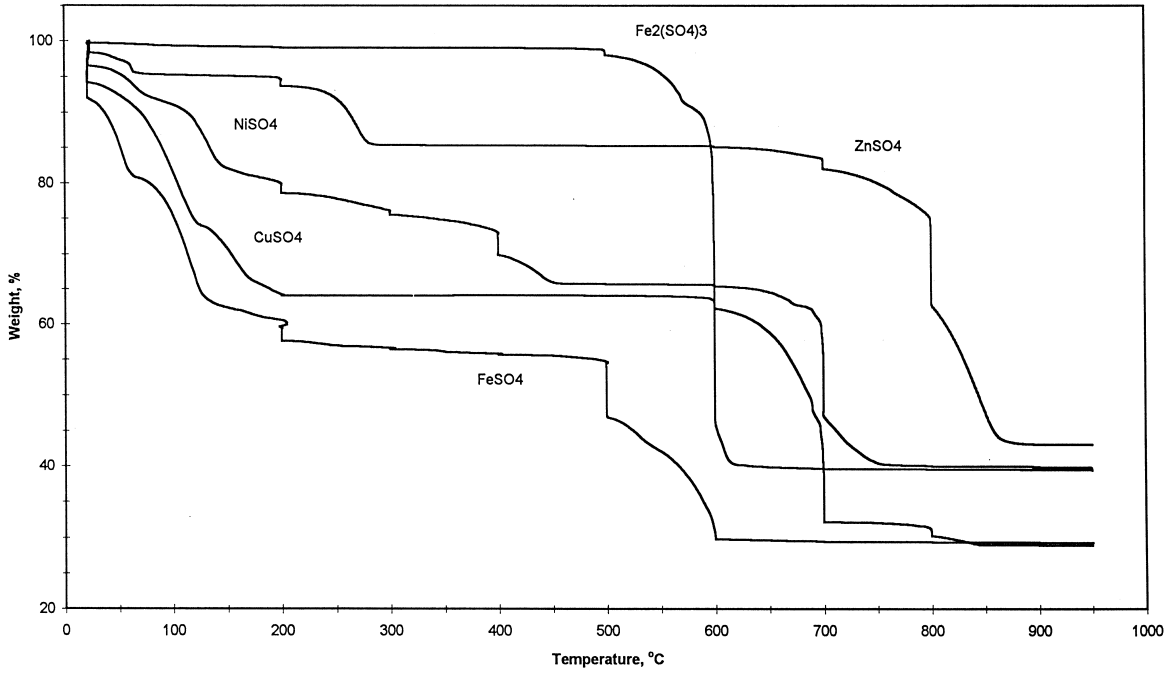

Fig. 1. TGA decomposition temperature profiles of metal sulfates.

Dehydration of nickel sulfate seems to occur between 50°C to 450°C. The initial decomposition of nickel sulfate seems to be rapid at 700°C, which was then followed by slow decomposition up to 750°C. Previous researchers have reported temperatures ranging from 675°C to 848°C for the decomposition of nickel sulfate. Complete decomposition was not observed. The TGA decomposition profile for $NiSO_4$ reached a minimum at 750°C and maintained that minimum through the maximum temperature of 950°C. The weight loss observed during decomposition was approximately 40%, corresponding to a stoichiometry of $NiSO_4 \cdot NiS + 2O_2$.

The decomposition temperature ranges for $Fe_2(SO_4)_3$ and $FeSO_4$ were similar as shown in Fig. 1. However, the shapes of the TGA decomposition curves were different. Initial dehydration for $FeSO_4 \cdot 7H_2O$ was observed at up to 200°C, with the decomposition of sulfate initiating around 500°C. There was a sharp decrease in weight at 500°C for $FeSO_4$, followed by a slower decomposition at 500°C–600°C. In contrast to this, $Fe_2(SO_4)_3$ started to decompose slowly at 500°C with a sharp decrease in weight around 575°C. The decomposition was complete at 600°C. Other researchers [12,13,19,20] observed a sharp decrease in weight due to decomposition in the temperature range of 550°C–625°C for $Fe_2(SO_4)_3$, which is similar to the temperature range observed in this work. Formation of intermediates during decomposition of iron sulfates has not been observed by previous researchers. Percent weight loss indicates a decomposition product of Fe_2O_3 for $Fe_2(SO_4)_3$ and FeO for $Fe(SO_4)$.

Initial dehydration of copper sulfate also occurs between 100°C to 200°C. Decomposition of copper sulfate initiates at 600°C, with a rapid change in weight observed around 675°C, as shown in Fig. 1. Decomposition proceeds more slowly between 700°C and 840°C, with the change in weight reaching a minimum at 840°C. The decomposition of copper sulfate in previous work has been reported in the range of 598°C to 625°C. Formation of oxysulfate intermediate has been observed by previous researchers [13,14,17]. Mu and Perimutter [13] reported that the initial decomposition temperature for copper sulfate was at 572°C, while the final decomposition was at 678°C. They observed higher initial (660°C) and final (740°C) decomposition tempera-

tures for the oxy-sulfate of copper than that for the copper sulfate. Percent weight loss indicates that complete decomposition has taken place and that the decomposition product is CuO.

Data indicates that decomposition was achieved in all samples tested, except for $NiSO_4$. Under the conditions used, the data for the decomposition of $NiSO_4$ eludes to formation of Metal Sulfate · Metal Sulfide + molecular oxygen. Such a reaction mechanism regarding the decomposition of $ZnSO_4$, $CuSO_4$, $Fe_2(SO_4)_3$ and $FeSO_4$ is also very possible, however the data obtained was insufficient to support the hypothesis.

3.2. X-ray diffraction data

X-ray diffraction (XRD) was conducted to identify the bulk crystalline phases formed during the decomposition. The X-ray diffraction data for the sulfates exposed to different temperatures are shown in Table 1. $FeSO_4$ completely converted to $Fe_2(SO_4)_3$ and Fe_2O_3 at 550°C. This may have contributed to the rapid decrease in the weight observed by TGA at 500°C, as shown in Fig. 1. At 600°C only Fe_2O_3 was observed, indicating that full decomposition had been achieved, which is consistent with the TGA data. However, in the TGA data, percent weight loss indicated a primary decomposition product of FeO. These discrepancies may result from that fact that the experiment conditions under which the samples were exposed were slightly different, with the samples decomposed in the TGA being exposed to a more reducing atmosphere. In contrast, $Fe_2(SO_4)_3$ only partially decomposed to Fe_2O_3 at 500°C and at 550°C, as shown in Table 1. The major species present was still $Fe_2(SO_4)_3$. In the decomposition of $Fe_2(SO_4)_3$, Fe_2O_3 did not become the dominant phase until 600°C, with $Fe_2(SO_4)_3$ not being completely converted to Fe_2O_3 until 650°C.

At 300°C, XRD data indicated the presence of only copper sulfate. At 650°C, a strong peak corresponding to oxysulfate [19] appeared, with this oxysulfate still present at 700°C. These temperatures are consistent with those observed with TGA. Complete transformation of $CuSO_4$ to CuO seems to take place around 750°C, according to the XRD data. Observation of the oxysulfate intermediate is consistent with observations by the previous researchers [17,19,20].

With nickel sulfate, XRD data indicated the presence of only $NiSO_4$ at temperatures up to 650°C. The NiO phase was not detected until 700°C, which is consistent with the decomposition temperatures observed with TGA data. Complete decomposition of $NiSO_4$ did not occur until 800°C. Phase changes in $NiSO_4$ were detected at 700°C, where the structure of $NiSO_4$ changes from monoclinic to tetragonal. As previously noted, complete decomposition of $NiSO_4$ to NiO was not observed in the TGA studies. Although the exact reasons for this are not known, it is strongly believed to result from the more reducing

Table 1
X-ray diffraction data of metal sulfates at different temperatures

Temp. (°C)	$FeSO_4$	$Fe_2(SO_4)_3$	$NiSO_4$	$CuSO_4$	$ZnSO_4$
300	$2Fe(OH)SO_4$, $Fe_2S_2O_9 \cdot XH_2O$	$Fe_2(SO_4)_3$	$NiSO_4 \cdot 6H_2O$	$CuSO_4$	$ZnSO_4 \cdot H_2O$
500	–	$Fe_2(SO_4)_3$, Fe_2O_3 – Low	–	–	–
550	Fe_2O_3, $Fe_2(SO_4)_3$	$Fe_2(SO_4)_3$ Fe_2O_3 – Low	–	–	–
600	Fe_2O_3	Fe_2O_3, $Fe_2(SO_4)_3$ – Low	–	–	$ZnSO_4 \cdot H_2O$
650	Fe_2O_3	Fe_2O_3	$NiSO_4$(Monoclinic), $NiSO_4 \cdot 6H_2O$	$CuO \cdot CuSO_4$ (oxysulfate), $CuSO_4$	$ZnSO_4 \cdot H_2O$
700	–	–	$NiSO_4$(tetragonal), $NiSO_4 \cdot 6H_2O$, NiO	$CuO \cdot CuSO_4$–Low, $CuSO_4$	ZnO
750	–	–	$NiSO_4$, NiO	CuO	ZnO
800	–	–	NiO	CuO	–

atmosphere the sample were exposed to during the TGA studies as well as the amount of total time that the samples were maintained at the given temperatures.

According to the XRD data, complete transformation of $ZnSO_4$ to ZnO seems to take place at 840°C. Previous researchers have observed an oxysulfate intermediate using XRD [11,15,18], but these intermediates were not observed during this study. No phase changes were reported during the decomposition of $ZnSO_4$ from the XRD analysis conducted in this study, which is in contrast to observations made by other researchers [11,15,18]. As in the case of $NiSO_{4,}$ these differences are strongly believed to result from the more reducing atmosphere that samples were exposed to during the TGA studies, as well as the amount of total time that the samples were maintain at a given temperature.

Intermediate products which could not be observed by XRD analysis maybe present in an amorphous forms. Their formation during the decomposition process cannot be excluded.

3.3. X-ray microanalysis

X-ray microanalysis was utilized in order to monitor the decomposition of the sulfate samples, which was indicated by the reduction in sulfur to metal ratio (S/[M]) as well as by the reduction in sulfur in the X-ray spectra. X-ray microanalysis was carried out using scanning electron microscopy/energy dispersive spectroscopy (SEM/EDS) and was performed on all samples, both fresh and those heated in the muffle furnace. Since the volume analyzed in X-ray microanalysis only contains a small portion of the top surface, the analysis obtained by this technique differs from that obtained by X-ray photoelectron spectroscopy (XPS). SEM/EDS analysis data is not necessarily representative of the sample bulk, as the penetration depth can be only a fraction of the sample depth. The penetration depth in electron microscopy is a function of several variables, among them accelerating voltage, beam current, and material type. In these series of experiments, the depth of the X-ray interaction volume, as computed by the Kanaya–Okayana equation [23], was approximately 0.7 μm, 0.74 μm, 0.76 μm, 1.1 μm, and 1 μm for the zinc, copper, nickel, iron (II) and iron (III) sulfates, respectively. The calculations were based on an average atomic number and atomic weight for each of the compounds, $n = 1.5$, and E_c equal to the characteristic energy of the Kα line of the heaviest element in the compound. Calculation of the depth of the X-ray interaction volume using Proza Curves software supplied with the Noran Instruments Voyager-4 Microanalysis system was approximately 2.0 μm, 2.0 μm, 1.9 μm, 2.3 μm, and 2.3 μm for the zinc, copper, nickel, iron (II) and Iron (III) sulfates respectively.

Plots of the sulfur to metal ratio (S/[M]) vs. temperature, of the metal sulfate samples are shown in Fig. 2, and are based on a weight percentage basis. The decomposition profiles of the Fe(II) and Fe(III) sulfates appear to be similar. The differences observed initially are due to the percentage of sulfur, iron, and oxygen initially present in the compounds. The degree of hydration is not expected to have any significant effect on the analysis, as the initial interaction of the electron beam with the sample will result in the removal of any adsorbed waters of hydration from the sample. The plots show that both Fe(II) and Fe(III) sulfate samples begin to decompose at approximately the same temperature, 500°C. Rapid decomposition of the Fe(II) and Fe(III) sulfates occurred at approximately 600°C, as indicated by the steep slope of the Fe(II) and Fe(III) sulfate decomposition curves in Fig. 2. These results are consistent with the bulk decomposition data obtained by TGA, as shown in Fig. 1.

Unlike the Fe(II) and Fe(III) sulfate samples, the decomposition profiles of the copper, nickel, and zinc sulfates differed, as shown in Fig. 2. The decomposition of the nickel sulfate proceeded fairly rapidly with increased temperature, once the decomposition process began. This was in contrast to the observations that were made of the copper and zinc sulfates, especially the zinc sulfate, where the decomposition of the sulfates occurred more gradually, as the temperature was increased. The initial decomposition temperature of the copper, nickel, and zinc sulfates, as shown in Fig. 2, are at approximately 550°C, 600°C, and 600°C, respectively. Rapid decomposition of the copper, nickel, and zinc sulfates began at approximately 700°C, 700°C, and 850°C, respectively. The results obtained here for the copper and nickel sulfates are consistent with the bulk de-

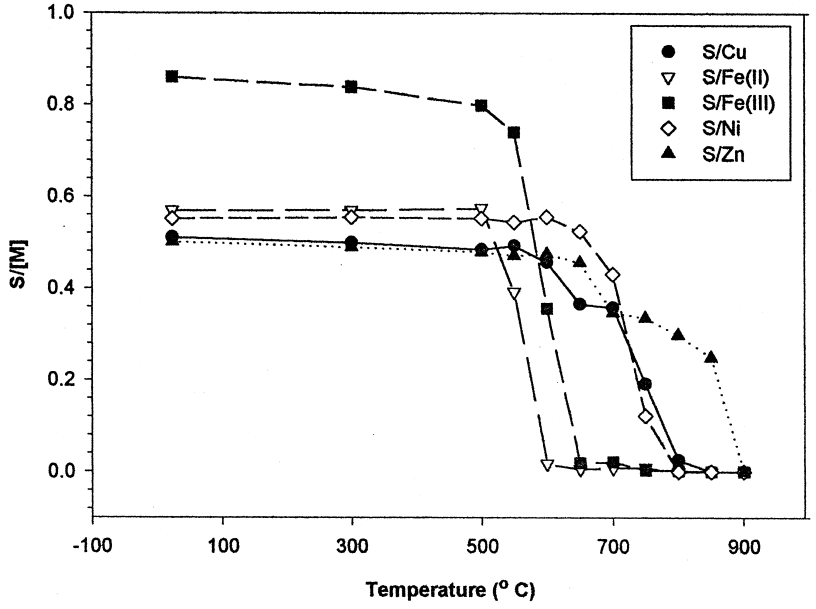

Fig. 2. X-ray microanalysis of sulfur/metal as a function of temperature.

composition temperature data observed by TGA, as shown in Fig. 1. The decomposition data obtained by SEM/EDS for the zinc sulfate differed considerably from that obtained with the TGA. Although initial decomposition appeared to take place at the same temperature, the profile of the decomposition curves differed. The decomposition curve obtained using TGA showed a sharp decrease at 800°C, while that obtained with SEM/EDS showed a more gradual change in slope, until 850°C, at which a sharp decrease was observed. The reason for this discrepancy is not completely understood, but maybe due to the fact that, with zinc sulfate, the sulfate concentration at the surface is not zero, even at the higher end of the decomposition temperature range (as observed by XPS and discussed in the next section) indicating that the sulfate at the surface is not fully depleted before the bulk decomposition. This non-zero surface component, although small compared to the total X-ray interaction volume, may still be significant enough to account for some of the differences in the profile of the decomposition curves of zinc sulfate.

The total decomposition temperature range, as determined by SEM/EDS, for copper, iron (II), iron (III), nickel, and zinc sulfates, as shown in Fig. 2, are approximately 550–850°C, 500–600°C, 500–600°C, 600–800°C, and 600–900°C, respectively. These decomposition temperatures are consistent with the bulk decomposition temperatures observed by TGA, as shown in Fig. 1, as well as with data reported in some of the literature [13,17,19,20,24]. The bulk decomposition temperature range, observed by TGA, although within the ranges observed with SEM/EDS, generally were narrower as compared to those observed with SEM/EDS. The narrower decomposition temperature range observed by TGA as compared to SEM/EDS may be due to the TGA instrument not being as sensitive to changes that are occurring at the surface and/or near surface, since it operates by recording changes in bulk weight. This observation may indicate that the changes in the sulfates, due to decomposition, initially occur near the surface. This observation is consistent with the suggestions obtained by other researchers [12,19], where it has been reported that, with metal sulfates, the decomposition occurs at the phase boundary between the undecomposed sulfate and the oxide product, and that the boundary proceeds uniformly from the surface towards the interior, a phenomena analogous to the sharp interface shrinking core models [25–28]. The decomposition process occurring along the phase boundary between the undecom-

posed sulfate and the oxide product is believed to result, at least in part, from the formation of a progressively thickening oxide product layer which creates an impedance effect. The impedance effect results from the constraint of diffusion imposed by the formation of the oxide product layer and possibly, to its recombination with SO_3 at the interface [12].

X-ray maps representative of the metal sulfate samples analyzed in these experiments are shown in Fig. 3. The X-ray maps show the relative sulfur distribution within a sample; the sulfur concentration, as represented by pixel intensity, cannot be inferred from the comparison of one X-ray map to another. X-ray maps of crystal cross sections, acquired for all metal sulfate samples, revealed no concentration gradients and/or a distinct phase boundary between the sulfate and oxide. The sulfur and the corresponding transition metal were observed to be uniformly distributed across the sample diameter. The non-observance of a concentration gradient and/or a distinct phase boundary between the sulfate and oxide in these experiments is not completely understood, but is believed to be due to a combination of effects.

For instance, it has been shown that the heating rate, in addition to total temperature, has a significant effect on decomposition and decomposition kinetics [13,18,29]. In addition, it is possible that over the duration of the heating period, the sample core obtained the same temperature as that of the sample surface, thereby facilitating a uniform distribution of the sulfur. It is unclear whether the thermal shock the samples under went by being placed into a pre-heated furnace, especially at elevated temperatures, contributed to this uniform distribution of sulfur.

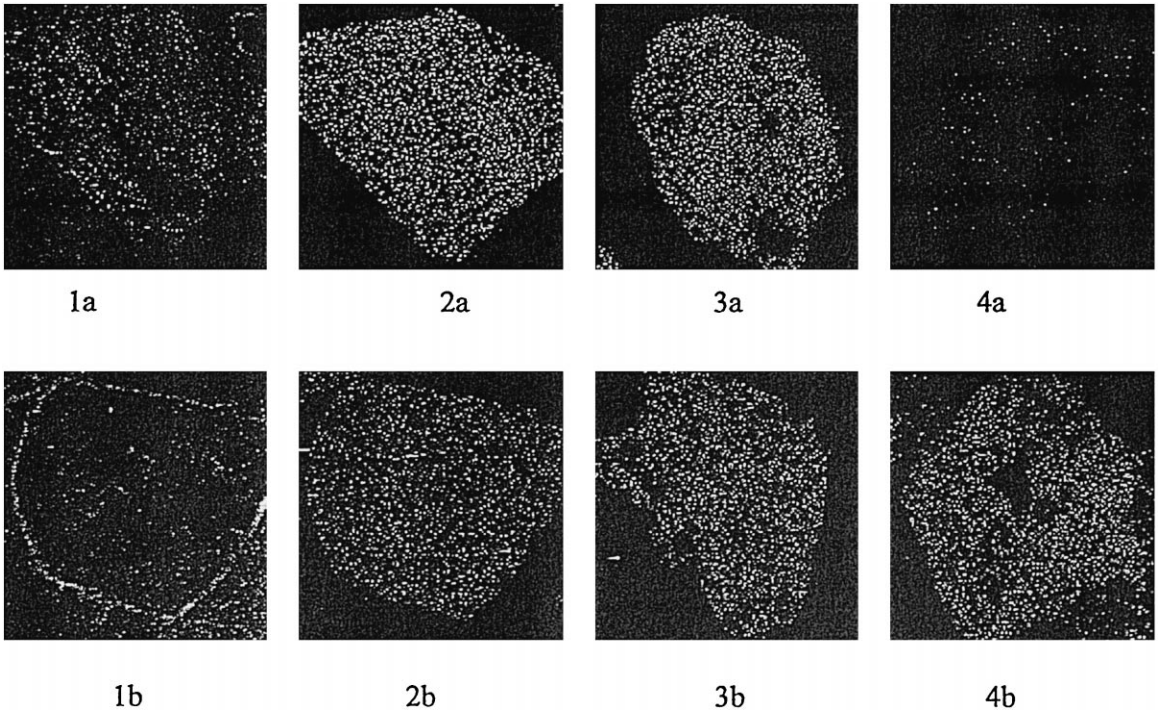

Fig. 3. X-ray microanalysis of sulfur distributions in iron (II) and nickel (II) sulfate. **Top: (1a)** Grey level image of unreacted Fe(II)SO_4 crystal; **(2a)** sulfur distribution of unreacted Fe(II)SO_4 crystal; **(3a)** sulfur distribution of Fe(II)SO_4 crystal heated to 600°C for 90 minutes; **(4a)** sulfur distribution of Fe(II)SO_4 crystal heated to 650°C for 90 minutes. **Bottom: (1b)** Grey level image of unreacted Ni(II)SO_4 crystal; **(2b)** sulfur distribution of unreacted Ni(II)SO_4 crystal; **(3b)** sulfur distribution of Ni(II)SO_4 crystal heated to 650°C for 90 minutes; **(4b)** sulfur distribution of Ni(II)SO_4 crystal heated to 700°C for 90 minutes.

3.4. X-ray photoelectron spectroscopic (XPS) analysis

XPS analysis was performed in order to understand the changes in the elemental composition and oxidation states of the elements at the surface (~ 50 Å). Similar studies have not being reported in the literature. The sulfur/metal ratios, shown in Fig. 4, were obtained by averaging the analysis of 3–6 data points obtained at a given temperature. The variation in the data from the average was approximately 25%, with the deviation becoming more apparent as the decomposition temperature was approached. This deviation indicates that the sulfur is not uniformly distributed on the surface during decomposition. Only the rapid changes in sulfur/metal ratio, observed when the temperature was increased, will be discussed here because of this large variation in the sulfur/metal ratio.

The ratios of sulfur/iron as a function of temperature obtained using the XPS data are shown in Fig. 4. The rapid change in the ratio of sulfur/iron for both Fe(III) sulfate and Fe(II) sulfate was observed in the temperature range of 500°C to 600°C. This is consistent with the TGA data, shown in Fig. 1 and the XRD data shown in Table 1. Therefore, the change in the surface of the iron sulfates during decomposition, as determined by XPS, is very similar to those of the bulk obtained by TGA.

The binding energies of sulfur for Fe(II) sulfate is around 169 ± 0.2 eV at room temperature. This corresponds to sulfur being in the sulfate form [30,31]. It is very interesting to note, that at 600°C, an additional sulfur peak was observed at 165.8 ± 0.2 eV, as shown in Fig. 5. The intensity of this secondary peak is higher at 600°C than that at 700°C. The peak deconvolutions, shown in Fig. 5, were obtained utilizing PHI Matlab program. The binding energy of the secondary peak is lower than that for sulfites (166.5–167 eV) [30,31] and higher than that for the elemental sulfur (~ 164 eV) [30,31]. Thus, the additional sulfur peak at 165.8 ± 0.2 eV may correspond to an oxidized form of sulfur. Formation of oxysulfate during the decomposition of iron sul-

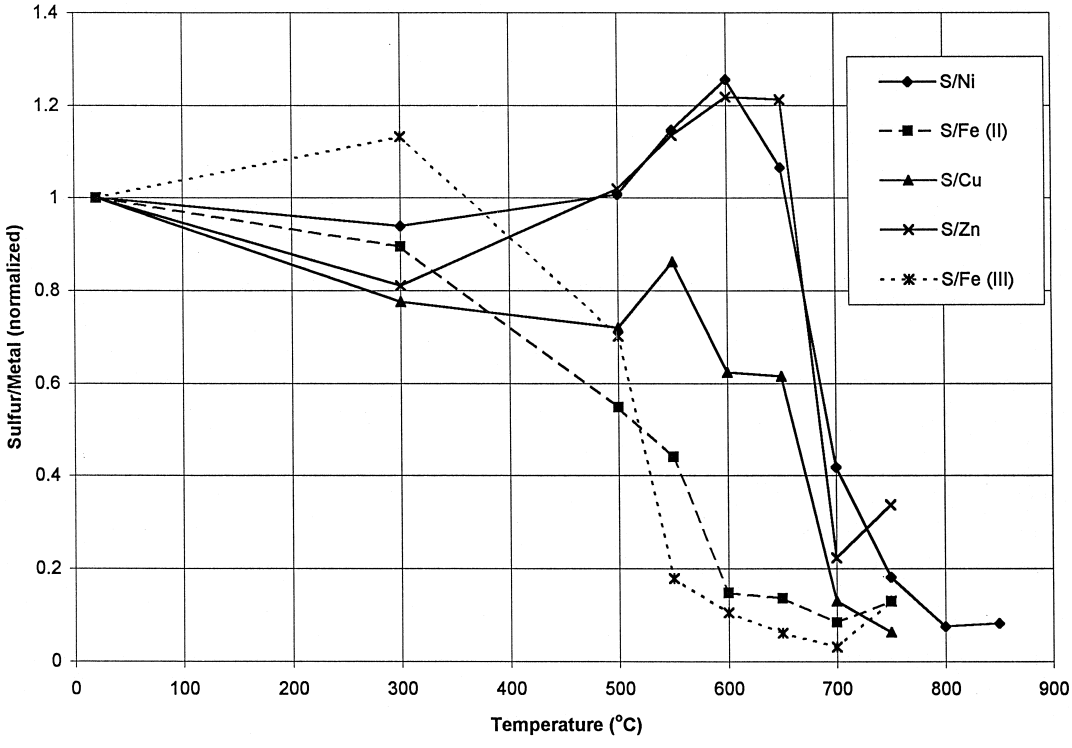

Fig. 4. XPS analysis of sulfur/metal as a function of temperature.

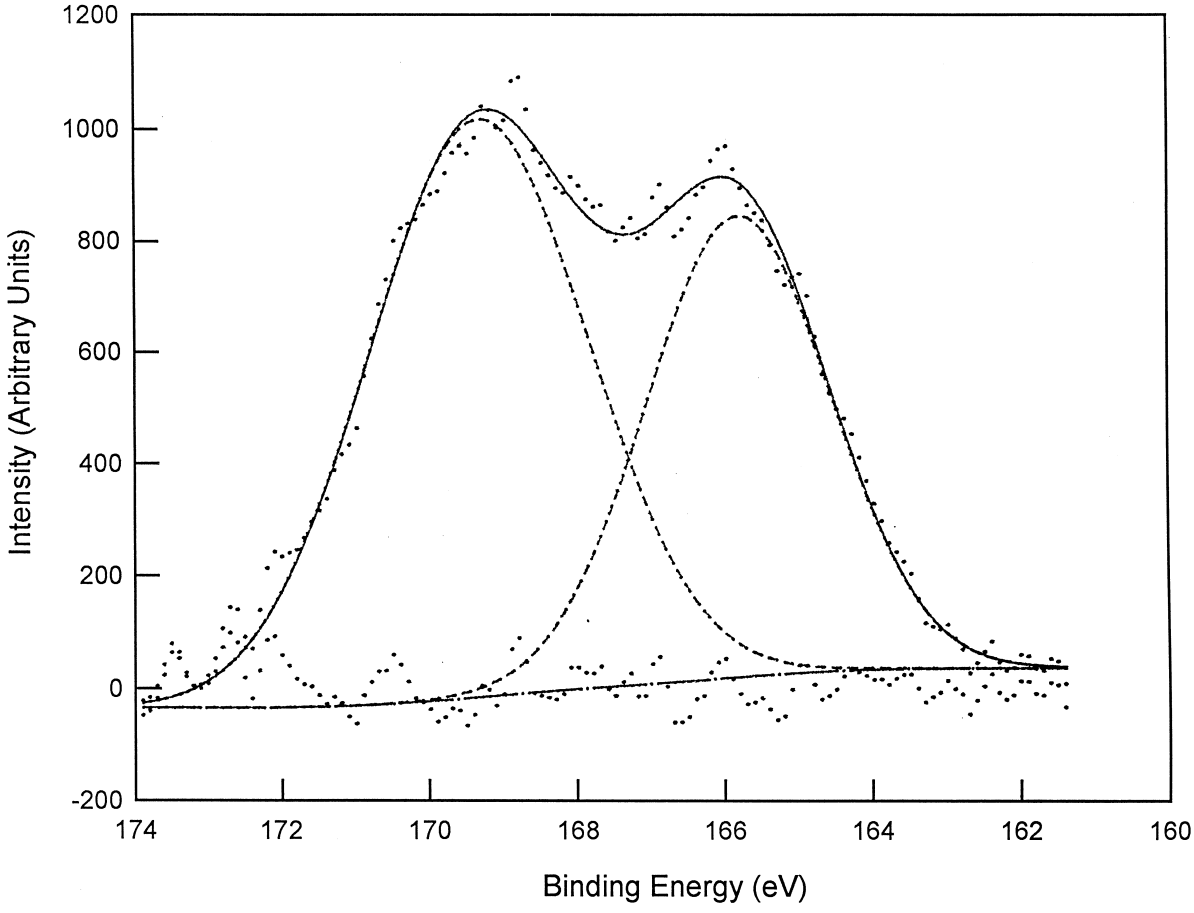

Fig. 5. Sulfur 2p spectrum of iron (II) sulfate heated to 600°C.

fates have not been reported by other researchers in the past. X-ray diffraction studies also did not indicate the presence of the oxysulfate structure. It is possible that this additional sulfur peak could be due to either adsorbed SO_3 formed during decomposition or the SO_3 type structure formed during the transformation of tetrahedral sulfate ion to a planer symmetric SO_3, molecule with a lower S–O bond length than that of sulfate.

The Fe 2p spectral region of Fe (II) sulfate at different temperatures is shown in Fig. 6. At room temperature the Fe $2p_{3/2}$ peak was broad with a binding energy of 711.6 eV. Broadening of the peak towards the higher binding energy side indicates that there is some Fe (III) species present, in addition to Fe (II) species. At 500°C, the binding energy increases to 712.7, indicating the formation of additional Fe (III) species, with the Fe (III) species most likely being in the sulfate form. This is consistent with the XRD data in Table 1. However, at 700°C, the peak became narrow, with a binding energy of 711.6 eV. This is similar to the binding energy of Fe_2O_3 [30,31]. The decrease in binding energy from 712.7 eV at 500°C to 711.6 eV at 700°C may be associated with the exclusive formation of the oxide from sulfate. This is consistent with the XRD data, in which Fe_2O_3 was the only form that was observed above 600°C.

One sulfur peak, at a binding energy of 169.0 ± 0.2 eV, corresponding to sulfate was observed for iron (III) sulfate at room temperature. At 550°C, an additional small sulfur peak was observed at 165.5 ±

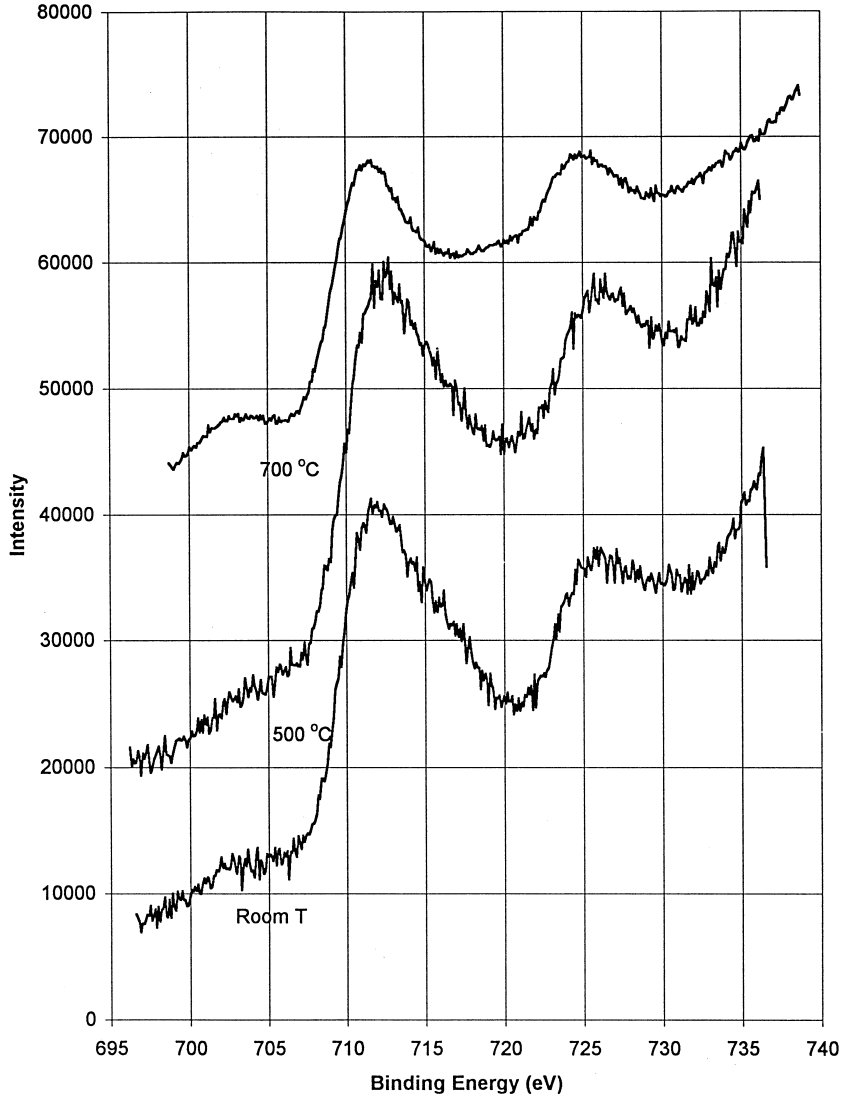

Fig. 6. Iron 2p spectra of iron (II) sulfate at different temperatures.

0.2 eV. The intensity of this additional peak at 165.5 ± 0.2 eV increased at 700°C. The sulfur 2p spectrum at 700°C is shown in Fig. 7. The binding energy of the secondary peak is very similar to that observed with iron (II) sulfate in Fig. 5, corresponding to an oxidized form of sulfur. Dissociation of iron (III) sulfate was observed around 500°C–600°C, as shown in Figs. 1, 2 and 4. Thus, the formation of this additional oxidized form of sulfur is hypothesized to be due to the dissociation of the sulfate. The Fe $2p_{3/2}$ peak at room temperature is broad with a binding energy of 712.6 ± 0.2 eV. At 550°C the binding energy shifts to a lower value of 711.7 eV, with the peak width becoming narrower as compared to that at room temperature. The lowering of binding energy may be associated with the formation of oxide. The XRD data indicated there is a substantial amount of Fe_2O_3 present after heating to 600°C. At 750°C, the binding energy of the Fe $2p_{3/2}$ peak is at 711.6 eV and the peak was broader, with an addi-

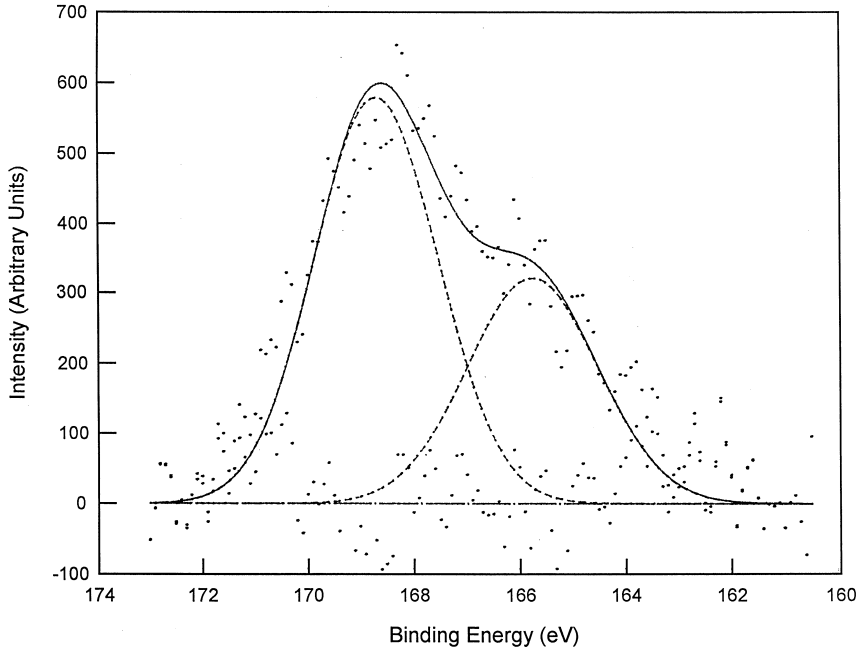

Fig. 7. Sulfur 2p spectra of iron (II) sulfate heated to 700°C.

tional peak (hump) around 708 eV. This indicates that there is some reduction of the iron (III) species at the surface when iron (III) sulfate was heated to high temperature. Some changes in the sulfur composition at the surface, as observed by X-ray photoelectron spectroscopy, occurred at a lower temperature than that of the more bulk changes observed with SEM/EDS and TGA, as shown in Fig. 4. However, the changes did not become dramatic until approximately 500°C, which is consistent with the observations made with SEM/EDS and TGA.

Sulfur/copper ratio data for the surface of copper sulfate, obtained using XPS are shown in Fig. 4. The major decrease in the ratio was observed at 600°C–700°C. The major weight change associated with bulk copper sulfate decomposition, as observed using TGA, was 600°C–700°C, as shown in Fig. 1. This value is consistent with that observed with XPS. The binding energy of the sulfur peak of copper sulfate was observed at 168.8 ± 0.2 eV, at room temperature. At 750°C two sulfur peaks at binding energies 166.2 eV (oxidized form of sulfur) and 168.9 eV (sulfate) were observed, as shown in Fig. 8. This is similar to the observations made with iron sulfate. Thus, the dissociation of copper sulfate is also accompanied with the formation of additional oxidized sulfur form. The Cu 2p spectra at different temperatures are shown in Fig. 9. At room temperature, the Cu 2p spectra contained satellite structures and the binding energy of the Cu $2p_{3/2}$ was at 933.4 eV. This binding energy value corresponds to Cu^{2+} type species. At 550°C the satellite structure decreased, as shown in Fig. 9, indicating that the there was some reduction of the Cu^{2+} species at 550°C. The Cu 2p spectra above 550°C was similar to that at 550°C. However, the bulk analysis of $CuSO_4$ at different temperatures, obtained from the XRD data, indicated only the presence of CuO, even at 750°C. Thus the species formed on the surface during the decomposition of $CuSO_4$ is different from those in the bulk.

Sulfur/nickel ratios at the surface for nickel (II) sulfate, at different temperatures, are shown in Fig. 4. The major decrease in the ratio was observed at 600°C–700°C. This is consistent with the data obtained for bulk decomposition with TGA, as shown in Fig. 1. The sulfur peak at room temperature corresponded to sulfate (168.9 eV). At 700°C an additional sulfur peak was observed at 166.8 eV, which is close to the binding energy of sulfite. This binding energy is slightly higher than the binding

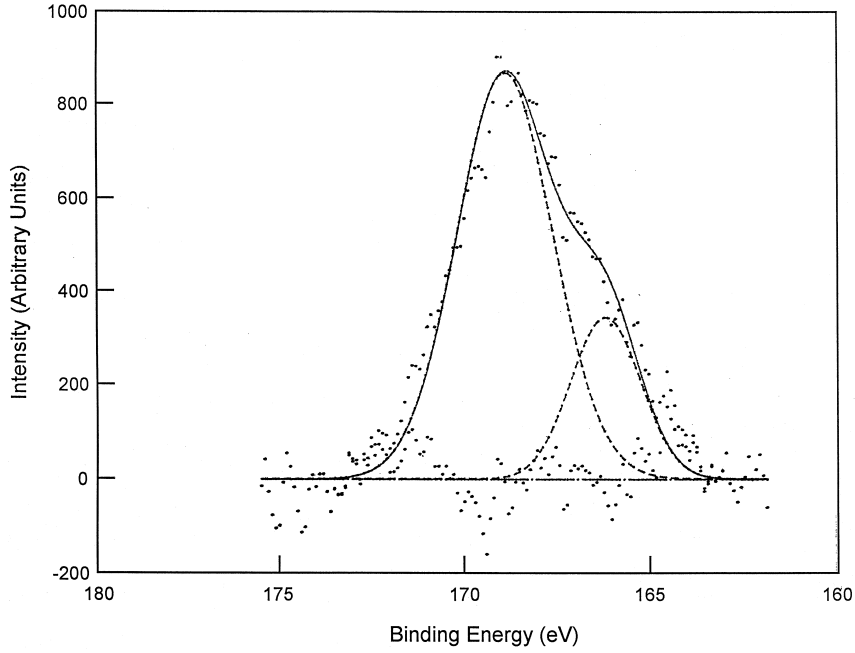

Fig. 8. Sulfur 2p spectra of copper sulfate heated to 750°C.

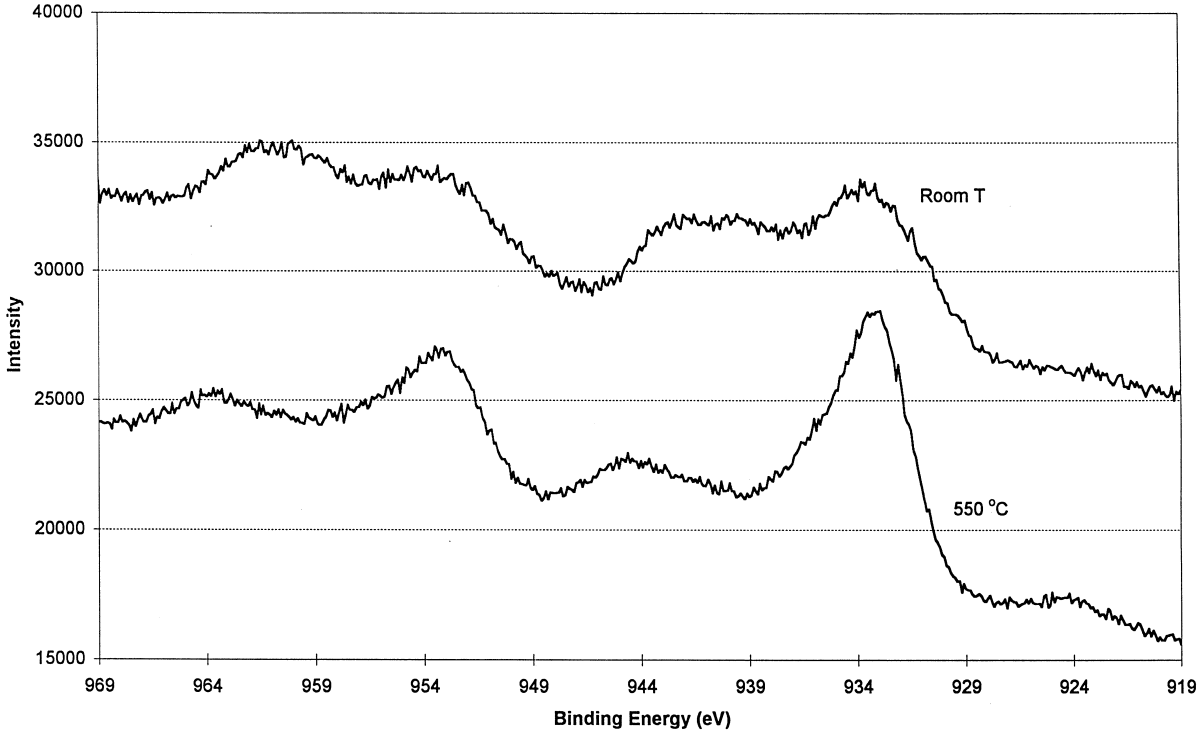

Fig. 9. Copper 2p spectra of copper sulfate at different temperatures.

energy of the secondary peak observed with iron at 500°C and with copper sulfate at 750°C. The dissociation of nickel observed at 600°C–700°C is also associated with the formation of a secondary sulfur peak. Nickel (2p) spectra at different temperatures are shown in Fig. 10. At room temperature the satellite peaks associated with the Ni $2p_{3/2}$ and Ni $2p_{1/2}$ were not well resolved, but at 800°C the satellite peaks were well resolved. The binding energy of the Ni $2p_{3/2}$ peak at 800°C was lower than that at room temperature. The shift in the binding energy to a lower value at 800°C may be associated with the formation of the nickel oxide, since nickel, in the oxide form, has a lower binding energy than that of the sulfate form [21].

The sulfur to zinc ratios at the surface of zinc sulfate, as measured by XPS, as a function of temperature are shown in Fig. 4. The major change in the ratio was observed at temperature 600°C–700°C. This is very consistent with the observations made with TGA, for the bulk decomposition of zinc sulfate, as shown in Fig. 1.

In all the metal sulfates, except for zinc sulfate, a secondary sulfur peak was observed in addition to the sulfate peak at the corresponding decomposition temperatures. The binding energy of this secondary sulfur peak was higher than that for elemental sulfur or sulfide but slightly lower than that for sulfite. This indicates that it corresponds to an oxidized form of sulfur, a structure which may be close to that of sulfite. It has been reported in the past [14,16] that gaseous SO_3 is initially formed during the decomposition, with the decomposition reaction usually starting at the outer surface.

Sulfate is originally in the tetrahedral form. During the initial formation of SO_3, the sulfate has to be converted to a weakly bonded SO_3 structure as shown below.

$$\text{Metal–SO}_4 \rightarrow \text{Metal–O} \rightarrow \text{SO}_3$$

Since the decomposition of sulfate initiates at the surface, formation of this $\text{M–O} \rightarrow \text{SO}_3$ structure should be observed at the initial stages of decomposition. However, this secondary sulfur form was only

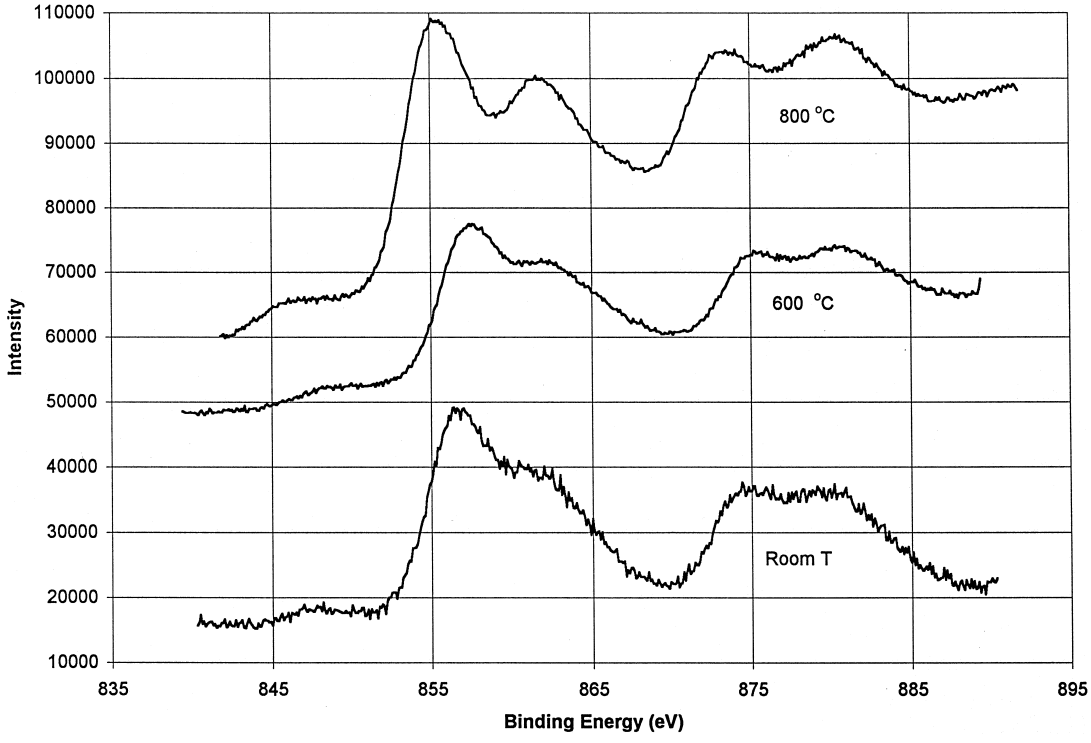

Fig. 10. Nickel 2p spectra of nickel sulfate at different temperatures.

observed at the higher end of the decomposition temperature range. For example, the decomposition temperature range for both $FeSO_4$ and $Fe_2(SO_4)_3$ is 500°C–600°C (Figs. 1 and 2). The secondary sulfur peak was observed at 600°C and 700°C respectively. For copper sulfate, the decomposition temperature range is 600°C–850°C, with the secondary sulfur peak being observed at 750°C. Similarly for nickel, sulfate the decomposition temperature range is 600°C–800°C, with the secondary form of sulfur being observed at 700°C. Thus, it is unlikely that this secondary form is due to the M–O → SO_3 structure formed at the initial stages of the decomposition.

After the decomposition, the surface of the metal sulfate exists in the oxide form. SO_3 that is formed in the bulk has to diffuse through the oxide layer at the surface before it is removed. The SO_3 formed in the bulk may be adsorbed on the metal oxide at the surface to form a ''Metal–O → SO_3'' type structure, and that may be the reason for the observation of the secondary peak at the higher end of the decomposition temperature range. It is possible that this adsorbed SO_3 type structure is unstable for ZnO and that may be the reason why this was not observed for $ZnSO_4$. Sulfate at the surface is not zero even at the higher end of the decomposition temperature range. This indicated that the sulfate at the surface is not fully depleted before the initiation of the bulk decomposition.

3.5. DRIFTS analysis

Diffuse reflectance infrared Fourier transform spectroscopy (DRIFTS) was carried out in order to both observe the decomposition of the metal sulfates in situ, as well as, to observe the effect of vacuum on the decomposition process. Similar studies have not been reported in the literature. In this DRIFTS study, system limitations precluded the analysis below 600 cm^{-1}. Zinc sulfide was used as the background/reference material. The spectroscopic region corresponding to sulfate was ratioed to zinc sulfide for all metal sulfates tested. The spectra obtained at each temperature was ratioed to that obtained at the previous temperature to determine the changes that occurred during the heating.

In all cases, the decomposition temperature observed in the DRIFTS study was lower than that observed with other techniques at atmospheric pressure. The decomposition of $FeSO_4$, as observed by DRIFTS, was between 300°C and 400°C. For $CuSO_4$, $NiSO_4$, and $ZnSO_4$, decomposition was observed between 550°C and 600°C. The effect of the vacuum, 10^{-5} Torr (1.3×10^{-3} Pa), in this series of experiments had the effect of lowering the initial decomposition temperature between 50°C and 100°C.

The initial spectra obtained for copper sulfate consisted of a series of distinct peaks over a broad region of 800 cm^{-1} to 1250 cm^{-1}. As the temperature was increased, a broad peak formed in the region of 1025 cm^{-1} to 1250 cm^{-1}, which encompassed the previously distinct peaks. At 400°C (as ratioed to that at 300°C) an increase in the intensity of the sulfate peak was observed. The increase in the intensity of the sulfate peak is speculated to be due to a rearrangement of the copper sulfate structure. As the temperature was further increased, the peak height of the sulfate peak decreased incrementally until 600°C (as ratioed to that at 550°C), where a large decrease in intensity of the sulfate peak was observed, indicating complete or near complete decomposition. It was also observed that at this temperature, the broad peak in the region 1025 cm^{-1} to 1250 cm^{-1} formed a doublet, with one band located between 1050 cm^{-1} to 1175 cm^{-1} and the second band between 1175 cm^{-1} and 1250 cm^{-1}. The centroid of the two broad peaks appear at 1209 cm^{-1} and 1140 cm^{-1}, Fig. 11 (the band above the base line indicates the species lost during heating). The region centered at 1209 cm^{-1} and 1140 cm^{-1} correspond to regions that have been identified by other researchers [32–34] as being due to adsorbed SO_2 and sulfate, respectively. It is possible that the two regions identified above, with centroids at 1209 cm^{-1} and 1140 cm^{-1}, may themselves contain multiple peaks.

The initial spectra obtained for zinc sulfate consisted of a series of distinct peaks within the range 950 cm^{-1} to 1250 cm^{-1}. As the temperature was increased, the series of distinct peaks in the sulfate region began to coalesce, forming a broad peak in the range 950 cm^{-1} to 1250 cm^{-1} and centered approximately around 1130 cm^{-1}. It was also observed during this period that there was a reduction in intensity of the sulfate band. As the temperature was further increased, no major changes in the spec-

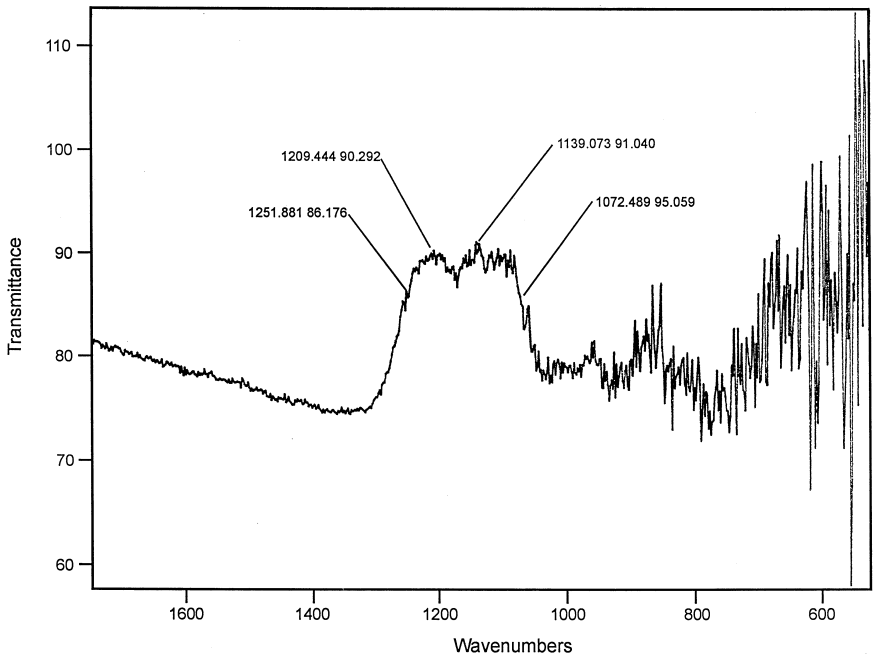

Fig. 11. DRIFTS spectra of copper sulfate at 600°C/550°C.

tra were observed until 600°C (ratioed to that at 550°C), where a large decrease in the intensity of the sulfate band was observed.

The spectra for iron (II) sulfate was similar to that of zinc sulfate both in its behavior and in the sense that the initial spectra consisted of a series of distinct peaks within the range 950 cm^{-1} to 1250 cm^{-1}. As the temperature was increased, the series of distinct peaks in the sulfate region began to coalesce, forming a broad peak in the range 950 cm^{-1} to 1250 cm^{-1} and centered approximately around 1135 cm^{-1}. As with zinc sulfate, a reduction in the sulfate band was also observed. A major change was observed at 400°C (as ratioed to that at 300°C), as indicated by a large decrease in peak height. The results obtained for the iron (III) sulfate were inconclusive. Despite repeated attempts, the experimental results obtained were not reasonable and did not correspond to any type of known decomposition process. Subsequently, no conclusion could be made regarding the results.

The initial spectra for Nickel sulfate, consisted of a series of small, widely separated, distinct peaks with in the range 800 cm^{-1} to 1200 cm^{-1}. As the temperature was increased, a broad peak formed in the range 900 cm^{-1} to 1250 cm^{-1}. As the temperature was further increased, the broad peak became broader and the spectral peak features less distinct. Changes in the sulfate peak were observed at 550°C (as ratioed to that at 500°C), with major changes being observed at 600°C (as ratioed to that at 550°C).

The effective lowering of the decomposition temperature under vacuum conditions was anticipated. Experimentally, the effective lowering of the decomposition temperature under vacuum conditions is simply a result of Le-Châtelier's Principal of equilibrium shift. As sulfate decomposition is an endothermic process, the application of heat to the sample (reactant) will tend to drive the decomposition reaction toward the right, favoring the formation of SO_2 (product). The turbomolecular pump attached to the DRIFTS cell effectively removes the SO_2 (product), driving the decomposition reaction further to the right in order to re-establish equilibrium and thereby facilitating the production of more SO_2.

Particle migration is an activated process, dependant upon variables such as system temperature and pressure. During the decomposition of sulfate, the SO_2 and/or SO_3 produced in the bulk has to diffuse

through the oxide product layer to the surface. When the external pressure at the surface, which acts like a ''retarding force'', is lowered, the pressure gradient between the bulk and surface increases. This increased pressure gradient enhances the diffusion of SO_2 and/or SO_3 to the surface. The enhanced diffusion and the resulting migration of SO_2 and/or SO_3 from the surface facilitates the decomposition process and decomposition occurs at a lower temperature.

Correspondingly, as system pressure is increased, increased temperature is required for decomposition to take place. It is hypothesized that the effect of pressure in limiting the rate at which the evolved SO_2 and/or SO_3 can diffuse through the system may result in the SO_2 and/or SO_3 re-reacting with the metal oxide to reform the metal sulfate. The re-reaction of SO_3 with the sample material has been postulated by other researchers [35,36].

4. Summary

1. Decomposition temperatures as observed by TGA in this study, at atmospheric pressure, were similar to those obtained by other researchers.
2. The decomposition characteristics of the bulk sample do not necessarily reflect the decomposition characteristics of the sample surface.
3. In all metal sulfates, except zinc sulfate, a secondary peak was observed on the sample surface in addition to the sulfate peak at the corresponding decomposition temperature. The binding energy of the secondary peak was higher then that for elemental sulfur or sulfide, but slightly lower than that for sulfite.
4. The secondary sulfur peak seen in all metal sulfates, except zinc sulfate, corresponding to an oxidized form of sulfur, was observed at the higher end of the decomposition temperature range.
5. Sulfate at the surface was not fully depleted before the initiation of the bulk decomposition, as observed by XPS.
6. A reduction in the oxidation state of the Cu^{2+} species was observed at 550°C and above. XRD data indicated only the presence of CuO, even at 750°C. This indicated that the surface of copper sulfate was different from that of the bulk during decomposition.
7. XRD data indicated the presence of copper oxysulfate between 650°C and 750°C. The presence of oxysulfate was not detected by XRD on other metal sulfate samples studied.
8. The profile of the decomposition curves obtained by SEM/EDS were not always representative of those obtained from TGA. This discrepancy results from that fact that TGA is a bulk analysis techniques, while that of the SEM is a near surface microanalysis technique.
9. X-ray mapping of the metal sulfates revealed no distinct oxide-sulfur interface during decomposition, under the experimental conditions used.
10. Vacuum had the effect of lowering the decomposition temperature of all metal sulfate samples, as compared to the decomposition temperature at atmospheric pressure, as observed by DRIFTS. Adsorbed SO_2 peak was observed during decomposition.

Acknowledgements

The authors would like to acknowledge the professionalism, ethics, and integrity of their various friends and colleagues during the past year.

References

[1] R.V. Siriwardane, Fixed bed testing of durable, steam tolerant zinc containing sorbents, Thirteenth Annual International Pittsburgh Coal Conference: Coal-Energy and the Environment Proceedings, 1, 1996, 590-595.
[2] J.A. Poston, A reduction in the spalling of zinc titanate desulfurization sorbents through the addition of lanthanum oxide, Ind. Eng. Chem. Res. 35 (3) (1996) 875–882.
[3] R.V. Siriwardane, U. Grimm, J. Poston, S.J. Monaco, Fixed Bed Testing of Durable, Steam Resistant Zinc Oxide Containing Sorbents, AIChE Annual Meeting, San Francisco, CA, Symposium on Gas Purification, Paper No. 247g, 1994.
[4] S. Lew, K. Jothimurugesan, M. Flytzani-Stephanopoulos, High temperature regenerative H_2S removal from fuel gases by regenerable zinc oxide–titanium dioxide sorbents, Ind. Eng. Chem. Res. 28 (1989) 535–541.
[5] T. Grindley, Desulfurization of Hot Coal gas by Zinc Ferrite, in: S.A. Newman (Ed.), Acid and Sour Gas Treating Processes, Chap. 16, Gulf Publishing, New York, 1984.
[6] T. Grindley, G. Steinfeld, Development and Testing of Regenerable Hot Coal–Gas Desulfurization Sorbent. Report,

DOE/METC/16545-1125; DOE/METC, Morgantowm, WV, 1981.
[7] R.V. Siriwardane, S. Woodruff, FTIR characterization of the interaction of oxygen with zinc sulfide, Ind. Eng. Chem. Res. 34 (2) (1995) .
[8] R.V. Siriwardane, J.A. Poston, G. Evans Jr, Spectroscopic characterization of molybdenum-containing zinc titanate desulfurization sorbents, Ind. Eng. Chem. Res. 33 (1994) 11.
[9] R.V. Siriwardane, J.A. Poston, Characterization of copper oxides, iron oxides, and zinc copper ferrite desulfurization sorbents by X-ray photoelectron spectroscopy and scanning electron microscopy, Applied Surface Science 68 (1993) .
[10] R.V. Siriwardane, J.A. Poston, Interaction of H_2S with zinc titanate in the presence of H_2 and CO, Applied Surface Science 45 (1990) .
[11] J.G. Ibanez, W.E. Wentworth, C.F. Batten, Chen, Kinetics of thermal decomposition of zinc sulfide, Rev. Int. Hautes Temp. Refract., Fr. 21 (1984) 113–124.
[12] G.A. Kolta, M.H. Askar, Thermal decomposition of some metal sulfates, Thermochimica Acta 11 (1975) 65–72.
[13] J. Mu, D.D. Perimutter, Thermal decomposition of inorganic sulfates and their hydrates, Ind. Eng. Chem. Process. Des. 20 (1981) 640–646.
[14] D.L. Hildenbrand, K.H. Lau, R.D. Brittan, Mechanistic aspects of metal sulfate decomposition process, High Temperature Science 26 (1990) 427–440.
[15] T.R. Ingrahm, H.H. Kellogg, Thermodynamic properties of zinc sulfate, zinc basic sulfate and system Zn–S–O, Transactions of Metallurgical Society of AIME 227 (1963) 1419.
[16] R.D. Brittain, K.H. Lau, D.R. Knittel, D.L. Hildenbrand, Effusion studies of the decomposition of zinc sulfate and zinc oxysulfate, J. Phys. Chem. 90 (1986) 2259–2264.
[17] H.H. Kellogg, A critical review of sulfation equilibria, Transactions of the Metallurgical Society of AIME 206 (1956) 1105–1111.
[18] R.N. Narayan, A. Tabatabaie-Raissi, M.J. Antal, A study of zinc sulfate decomposition at low heating rates, Ind. Eng. Chem. Res. 27 (1988) 1050–1058.
[19] H. Tagawa, H. Saijo, Kinetics of the thermal decomposition of some transition metal sulfates, Thermochimica Acta 91 (1985) 67–77.
[20] H. Tagawa, Thermal decomposition temperatures of metal sulfates, Thermochimica Acta 80 (1984) 22–33.
[21] C.D. Wagner, W.M. Riggs, L.E. Davis, J.F. Moulder, G.E. Muilenburg, Handbook of X-Ray Photoelectron Spectroscopy, in: G.E. Muilenburg (Ed.), Perkin-Elmer, Physical Electronics Division, Eden Priarie, MN, 1979.
[22] J.I. Goldstein, D.E. Newbury, P. Echlin, D.C. Joy, C. Fiori, E. Lifshin, Electron Beam Specimen Interactions, in: Scanning Electron Microscopy and X-ray Microanalysis, Chap. 6, Plenum, New York, 1981.
[23] J.I. Goldstein, D.E. Newbury, P. Echlin, D.C. Joy, C. Fiori, E. Lifshin, Electron Beam Specimen Interactions, in: Scanning Electron Microscopy and X-ray Microanalysis, Chap. 3, Plenum, New York, 1981.
[24] R. Weast (Ed.) Handbook of Chemistry and Physics, 64th edn., Section B, The Chemical Rubber, Cleveland, OH, 1983.
[25] J. Szekely, J.W. Evans, Chem. Eng. Sci. 26 (1971) 1901.
[26] H.Y. Sohn, Szekely, J. Chem. Eng. Sci. 27 (1972) 763.
[27] J. Szekely, J.W. Evans, H.Y. Sohn, Gas–Solid Reactions, Chap. 3, Academic Press, New York, 1976.
[28] G.D. Focht, P.V. Ranade, D.P. Harrison, High-temperature desulfurization using zinc ferrite: regeneration kinetics and multicycle testing, Chem. Eng. Sci. 44 (12) (1989) 2919–2926.
[29] O.H. Krikorian, P.K. Shell, The utilization of $ZnSO_4$ decomposition in thermochemical hydrogen cycles, Int. J. Hydrogen Energy 7 (6) (1982) 463–469.
[30] R.V. Siriwardane, J. Cook, Interaction of SO_2 with iron deposited on CaO(100), Journal of Colloid And Interface Science 116 (1) (1987) .
[31] R.V. Siriwardane, Interaction of SO_2 and O_2 mixtures with CaO and sodium deposited CaO, Journal of Colloid and Interface Science 132 (1) (1989) .
[32] R.V. Siriwardane, S. Woodruff, In-situ fourier transform infrared characterization of sulfur species resulting from the reaction of water vapor and oxygen with zinc sulfide, Ind. Eng. Chem. Res. 36 (12) (1997) .
[33] P.H. Berben, M.J. Kappers, J.W. Geus, An FT-IR study of adsorption of sulfur dioxide on alpha- and gamma-alumina, Mikrochimica Acta II (1988) .
[34] M.A. Martin, J.W. Childers, R.A. Palmer, Fourier transform infrared photoaccoustic spectroscopy characterization of sulfur–oxygen species resulting from the reaction of SO_2 with CaO and $CaCO_3$, Applied Spectroscopy 4 (1987) .
[35] V.E. Steger, W. Schmidt, Infrarotspektren von sulfaten und phosphaten fur physikalishe chemie, Ber. Bunsen-Ges. Phys. Chem. 68 (1964) .
[36] R.B. Fahim, G.A. Kolta, J. Phys. Chem. 74 (1970) .